

NUMERICAL MODELING OF THE ULTRASONIC CAVITATION FIELD AND EXPERIMENTAL EVALUATION OF BUBBLE DENSITY

PACS REFERENCE: 43.35 E1

B. Dubus¹, C. Granger¹; P. Mosbah¹; A. Moussatov¹, H. Schmit¹; L. Sztor¹; C. Campos-Pozuelo²

¹ IEMN département ISEN, UMR CNRS 8520, 41 boulevard Vauban, 59046 Lille Cedex, France
email: dubus@isen.fr

² Instituto de Acustica, CSIC, Serrano 144, 28006 Madrid, Spain
email: ccampos@ia.cetef.csic.es

ABSTRACT

A numerical model of ultrasonic cavitation field is described. It is based on a phenomenological description of a cavitating fluid as a non linear fluid whose characteristics (sound speed, density) depend upon the bubble density. To obtain the constitutive relationship between bubble density and acoustic pressure, a real-time measurement method of the bubble density, relying upon the variation of the electrical resistance of the medium, is proposed. The finite element formulation of the model is derived and implemented in the ATILA code. Computational results on the cavitation field created by a cylindrical concentrator are presented.

INTRODUCTION

The development of industrial devices using physical and chemical processes assisted by ultrasonic cavitation is constrained by the limitation of existing modeling. This difficulty is due to the fact that processes involved are highly non linear and the reactions taking place in the fluid cannot be described by simple mathematical relations. More over, the overall efficiency of devices using cavitation is usually low and an oversizing cannot easily compensate for a bad design. Numerical modeling can provide the tools that would help to optimize the design of these devices.

The development of these numerical models involves different scales: the reactor scale corresponding to the parameters (reactor geometry, transducer...) available to the designer, the bubble scale where most physical processes (vibration, rectified diffusion, coalescence, fragmentation, Bjerknes forces...) take place; the particle scale used to describe the cavitating fluid as a continuum. The microscopic non linear phenomena must be translated into a constitutive equation (at the particle scale) in order to be implemented in the numerical model. Existing numerical models [1-4] start from the study of the dynamical behavior of the single bubble. Strong hypotheses (linear vibration [2, 3], isolated bubbles [1-4], prescribed distribution of bubble sizes [1-4], no coalescence or fragmentation [1-4]) are then added. Finally, the Caflish model [5] is used to build up a constitutive equation of the cavitating fluid. Resulting equations are expressed in the time-domain and solved using finite element [1] or finite difference [2-4] methods.

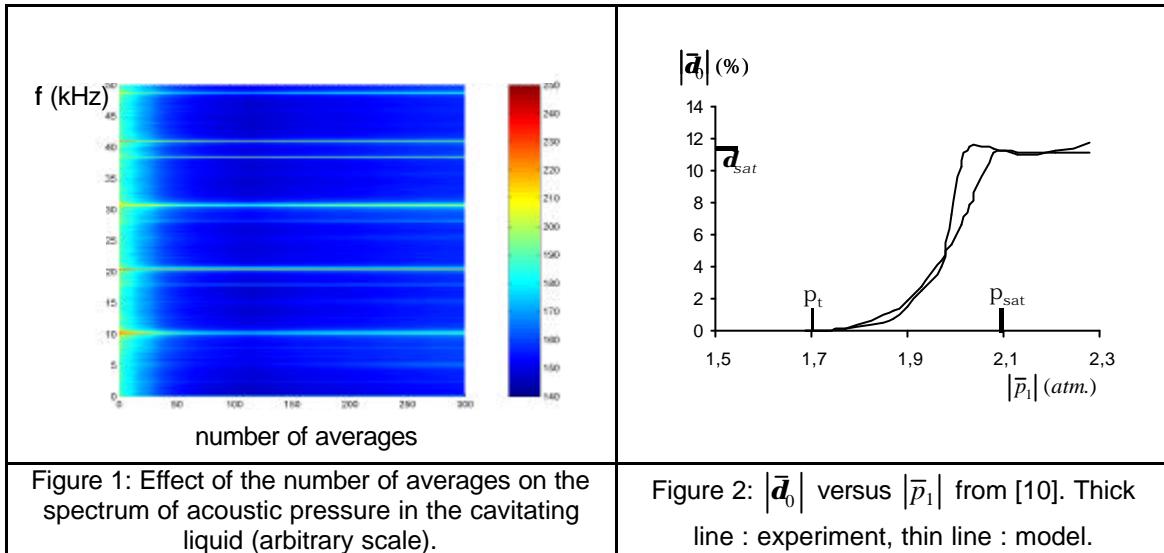
A different approach is presented here. Firstly, it is assumed that the cavitating fluid reaches a steady-state. Physical quantities are described by their average value at the working frequency.

Secondly, bubbles at the particle level are represented by an additional macroscopic variable, the bubble density. Thirdly, a phenomenological law relating pressure to bubble density is assumed. This law takes into account, in steady-state, the overall balance between nucleation, bubble vibration, rectified diffusion, fragmentation and coalescence.

1. MODEL

1.1. Stationnarity

The first hypothesis of the proposed model assumes the existence of a stationary state in the reactor. To verify this assumption, pressure measurements are performed in a probe reactor using a longitudinal horn-type transducer whose radiating surface is located at the free surface of a water tank. Successive pressure acquisitions of 0.1 s are made with a sampling frequency of 100 kHz. The frequency spectrum of each acquisition is evaluated by a Discrete Fourier Transform and then successive spectra are averaged. Figure 1 displays the influence of the number of averages on the frequency spectrum. After, 40 to 50 averages, the stochastic character of the pressure disappears and the average spectrum is obtained. Lines in the spectrum are associated to the fundamental frequency at 20.5 kHz, as well as higher harmonics and sub-harmonics resulting from non linear bubble vibration. When the pressure is monitored over a longer duration with an averaging over 40 acquisitions, the spectral amplitude at the fundamental frequency varies within 2 dB [6]. This result shows that the hypothesis of stationnarity used in the model is realistic.



1.2. Conservative and state equations

The bubble density $\mathbf{d}(\mathbf{r}, t)$ is defined as the volume fraction of bubbles. In steady-state, the maximum value of \mathbf{d} is well-known as cavitation index [7, 8]. At the particle scale, the equations of the model are the conservation of mass

$$\frac{\partial \mathbf{r}}{\partial t} + \text{div}_{\mathbf{r}_0} \mathbf{v} = 0, \quad (1)$$

the conservation of momentum

$$\mathbf{r}_0 \frac{\partial \mathbf{v}}{\partial t} + \text{grad } p = \mathbf{0}, \quad (2)$$

and the state equation

$$\mathbf{r} - \mathbf{r}_0 = \frac{p}{c_0^2} - \mathbf{r}_0 \mathbf{d}. \quad (3)$$

\mathbf{r} and \mathbf{r}_0 are respectively the density and the initial density, \mathbf{v} is the particle velocity, p is the pressure, c_0 is the speed of sound in the liquid and t is the time. Equations (1) to (3) are combined to obtain

$$\Delta p - \frac{1}{c_0^2} \frac{\partial^2 p}{\partial t^2} = -\mathbf{r}_0 \frac{\partial^2 \mathbf{d}}{\partial t^2} . \quad (4)$$

The Ritz averaging method [9] applied to eq. (4) allows to obtain an approximate steady-state solution. The approximated values of pressure \tilde{p} and bubble density $\tilde{\mathbf{d}}$ are written

$$\tilde{p}(\mathbf{r}, t) = \sum_{n=1}^N (p_{1n}(\mathbf{r}) \cos n\mathbf{w} + p_{2n}(\mathbf{r}) \sin n\mathbf{w}) = \sum_{n=1}^N \bar{p}_n(\mathbf{r}) e^{+jn\mathbf{w}} , \quad (5)$$

$$\tilde{\mathbf{d}}(\mathbf{r}, t) = \sum_{n=1}^N (\mathbf{d}_{1n}(\mathbf{r}) \cos n\mathbf{w} + \mathbf{d}_{2n}(\mathbf{r}) \sin n\mathbf{w}) = \sum_{n=1}^N \bar{\mathbf{d}}_n(\mathbf{r}) e^{+jn\mathbf{w}} , \quad (6)$$

where \mathbf{w} is the angular frequency, \bar{p}_n and $\bar{\mathbf{d}}_n$ are the complex amplitudes of the spectral components of pressure and bubble density respectively. The Ritz averaging criterion states that the "best" approximate solution is obtained by canceling the integrals

$$\int_0^{2\pi/\mathbf{w}} \left(\Delta \tilde{p} - \frac{1}{c_0^2} \frac{\partial^2 \tilde{p}}{\partial t^2} + \mathbf{r}_0 \frac{\partial^2 \tilde{\mathbf{d}}}{\partial t^2} \right) \begin{pmatrix} \cos m\mathbf{w} \\ \text{or} \sin m\mathbf{w} \end{pmatrix} dt = 0 \quad (7)$$

The computation of the integrals leads to a set of uncoupled equations on the complex amplitudes of the spectral components:

$$\Delta \bar{p}_n + \frac{n^2 \mathbf{w}^2}{c_0^2} \bar{p}_n = \mathbf{r}_0 n^2 \mathbf{w}^2 \bar{\mathbf{d}}_n . \quad (8)$$

1.3. Phenomenological law

A constitutive relationship between the different spectral components \bar{p}_n and $\bar{\mathbf{d}}_n$ (where m can be different from n) is required to close the model. A first evaluation is carried out from measurements made by V.A. Akulichev [10] on the axis of a cylindrical ring transducer driven at 15.4 kHz. In this experiment, the change of volume measured by dilatometric method [7] (insertion of a capillary in the cavitation zone) is the amplitude of the "static" bubble density $|\bar{\mathbf{d}}_0|$.

The variation of $|\bar{\mathbf{d}}_0|$ with $|\bar{p}_1|$ is displayed in Figure 2. Three zones are shown:

$$|\bar{\mathbf{d}}_0| = \mathbf{a}(|\bar{p}_1|) = \begin{cases} 0 & \text{if } |\bar{p}_1| \leq p_t \\ \mathbf{b}(|\bar{p}_1| - p_t)^3 & \text{if } p_t \leq |\bar{p}_1| \leq p_{sat} \\ \mathbf{d}_{sat} & \text{if } |\bar{p}_1| \geq p_{sat} \end{cases} . \quad (9)$$

As long as the pressure is lower than the cavitation threshold p_t , there is no cavitation, and hence, the bubble density is set to zero. In the second zone where $p_t \leq |\bar{p}_1| \leq p_{sat}$, the bubble density varies with the acoustic pressure. This is an "unsaturated cavitation" where fragmentation effects dominate because of the low concentration of bubbles. In this zone, the number of bubbles per unit volume increases as the acoustic pressure increases [10]. When $|\bar{p}_1| \geq p_{sat}$, the bubble density reaches a maximum value of \mathbf{d}_{sat} . In this "saturated cavitation" zone, coalescence effects are predominant, resulting in a decrease of the number of bubbles per unit volume and an increase of the bubble size as pressure increases. In the real process, there is a continuous transition from unsaturated to saturated cavitation as the bubble density increases and the bubbles are getting less and less isolated. It can be noted that eq. (9) does not provide the relationship between the spectral components of pressure and bubble density needed in eq. (8). A new method for measuring spectral components of bubble density is described in section 3. In the following, only the components at the fundamental frequency are considered with the following relationship:

$$\bar{\mathbf{d}}_1 = \mathbf{a}_1(\bar{p}_1) , \quad (10)$$

where \mathbf{a}_1 is a complex function. After combining equations (8) and (10), the resulting equation is

$$\Delta \bar{p}_1 + \frac{\mathbf{w}^2}{c_0^2} \left[1 - \mathbf{r}_0 c_0^2 \frac{\mathbf{a}_1(\bar{p}_1)}{\bar{p}_1} \right] \bar{p}_1 = 0 . \quad (11)$$

According to the value of $\mathbf{a}_1(\bar{p}_1)$, the local solution can be purely a propagating wave, a purely attenuated wave, or a propagating wave with attenuation

1.4. Numerical model

The weighted residual (Galerkin) method is applied to eq. (11) together with the classical finite element discretization scheme. The discretized set of equation is

$$\left\{ \frac{1}{\mathbf{w}^2} [A_1] - [A_2] + [A_3(\mathbf{P})] \right\} \mathbf{P} = \mathbf{r}_0 \mathbf{U} \quad (12)$$

where \mathbf{P} and \mathbf{U} are the vectors of the nodal values of pressure and prescribed displacement (transducer surface) respectively with

$$[A_1] = \sum_e \iiint_{\Omega^e} [B^e] [B^e] d\Omega^e \quad (13)$$

$$[A_2] = \sum_e \iiint_{\Omega^e} [N^e] \frac{1}{c_0^2} [N^e] d\Omega^e \quad (14)$$

$$[A_3(\mathbf{P})] = \sum_e \iiint_{\Omega^e} \mathbf{r}_0 [N^e] \frac{\mathbf{a}_1\left(\frac{[N^e] \mathbf{P}^e}{[N^e] \mathbf{P}^e}\right)}{[N^e] \mathbf{P}^e} [N^e] d\Omega^e \quad (15)$$

$[N^e]$ and $[B^e]$ are the interpolation and the space derivative interpolation elementary matrices respectively and e denotes the finite element. Eq. (12) is solved by a two-steps procedure. Firstly, the linear pressure field \mathbf{P}_0 is computed for a prescribed displacement \mathbf{U}_0 corresponding to the cavitation threshold

$$\left\{ \frac{1}{\mathbf{w}^2} [A_1] - [A_2] \right\} \mathbf{P}_0 = \mathbf{r}_0 \mathbf{U}_0 \quad (16)$$

Then, an incremental resolution is performed using a tangent matrix method [11]

$$\left\{ \frac{1}{\mathbf{w}^2} [A_1] - [A_2] + [A_3(\mathbf{P}_n)] + \left[\frac{d[A_3]}{d\mathbf{P}}(\mathbf{P}_n) \right] \mathbf{P}_n \right\} \Delta \mathbf{P}_n = \mathbf{r}_0 \Delta \mathbf{U}_n \quad (17)$$

$$\mathbf{P}_{n+1} = \mathbf{P}_n + \tilde{\mathbf{A}} \mathbf{P}_n \quad (18)$$

This formulation is implemented in the finite element code ATILA [12] which can take into account piezoelectricity, fluid-structure coupling and acoustic radiation problems.

2. APPLICATION EXAMPLE: THE CYLINDRICAL CONCENTRATOR

A piezoelectric ring acting as a cylindrical concentrator is considered. The inner radius of the ring is 8 cm and the excitation frequency is 15.4 kHz. Due to the symmetry of the geometry, only 1° of the internal fluid cavity is meshed. The mesh is denser at the center of the cavity where cavitation is expected. In this zone, the wave velocity sharply decreases and the element length must be kept smaller than $\lambda/4$ (where λ is the wavelength). A displacement is prescribed at the inner radius of the ring. It is assumed that $|\bar{\mathbf{d}}_1|$ and $|\bar{p}_1|$ in equation (10) are related as $|\bar{\mathbf{d}}_0|$ and $|\bar{p}_1|$ in equation (9) and that $\bar{\mathbf{d}}_1$ and \bar{p}_1 have the same phase.

Figure 3 and 4 display the variation of acoustic pressure and bubble density versus radius for various prescribed displacement of the ring. Several effects are noted: *i)* the acoustic pressure saturates rapidly in the cavitation zone; *ii)* the size of the cavitation zone stays almost constant; *iii)* pressure nodes and antinodes are spatially shifted when the amplitude of displacement is increased. The computation is stopped when a second cavitation zone appears around $r = 4$ cm, requiring a refinement of the mesh.

3. MEASUREMENT OF THE BUBBLE DENSITY

The principle of the method is to measure the variation of the fluid electrical impedance due to the bubbles vibration. From an electrical point of view, the bubbles can be seen as insulating spheres of variable radius if the electrochemical effects of cavitation are neglected. The

vibration of the bubbles modifies the current density lines and therefore affects the impedance (mainly resistive) between two point electrodes.

The experimental device is presented in Fig. 5. The cavitation field is generated by a horn-type transducer at $f_{BF} = 20.5$ kHz. The probe is driven at high frequency ($f_{HF} = 89$ kHz) and small amplitude in order to avoid electrolytic and oxydo-reduction reactions. If R_1 is much larger than the probe resistance at the primary of the transformer, the relative variation of voltage V_2 is equal to the relative variation of the probe resistance. The real-time variation of the resistance is too small (typical relative variation of 10^{-3}) to be directly visualized. However, as the voltage V_2 is a high frequency signal whose amplitude is modulated by the bubble vibration, lines associated to the bubble vibration are found in the frequency spectrum, even for small relative variation (up to 10^{-4}). Fig. 6 displays the amplitude spectrum of V_2 averaged over 40 acquisitions and synchronized on the drive signal. Lines found at $f = f_{HF} - (n+1)f_{BF}$ ($n = 0$ to 3) i.e. 68.5, 48, 27.5 and 7 kHz and $f = (n+1)f_{BF} - f_{HF}$ ($n = 4$ to 6) i.e. 13.5, 34 and 54.5 kHz can be attributed to fundamental and higher harmonic of the bubble density variation. Parasitic lines are found at $f = (m+1)f_{BF}$ ($m = 0$ to 3) i.e. 20.5, 41, 61.5, and 82 kHz (electromagnetic radiation from transducer), and at 38 and 76 kHz (electromagnetic radiation from other apparatus). Other lines have still to be analyzed. Similar data can be obtained for the phase spectrum of V_2 . From these amplitude and phase information, the average time-variation of the bubble density can be reconstituted.

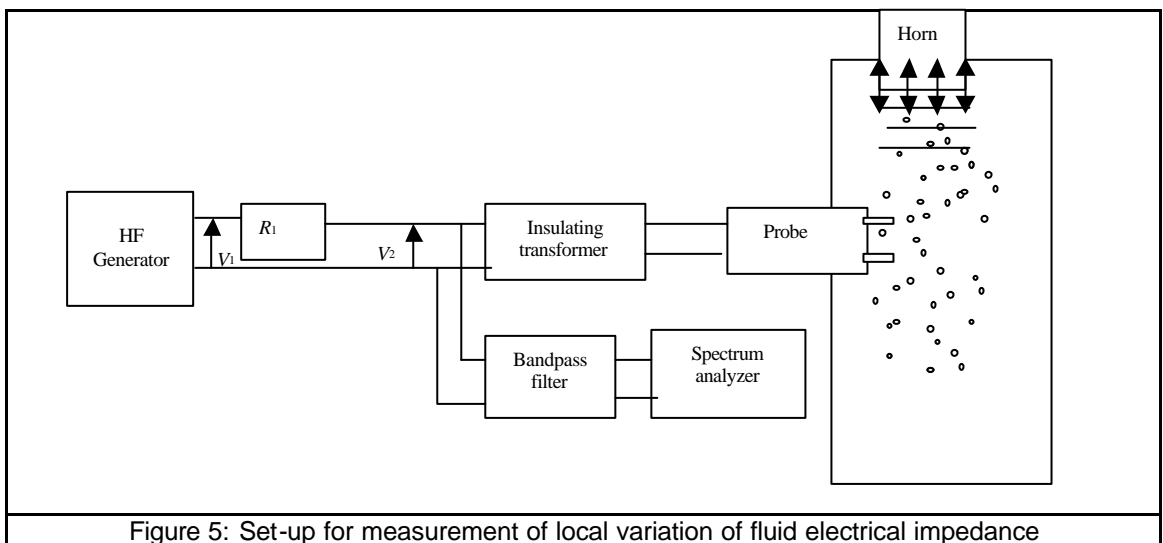
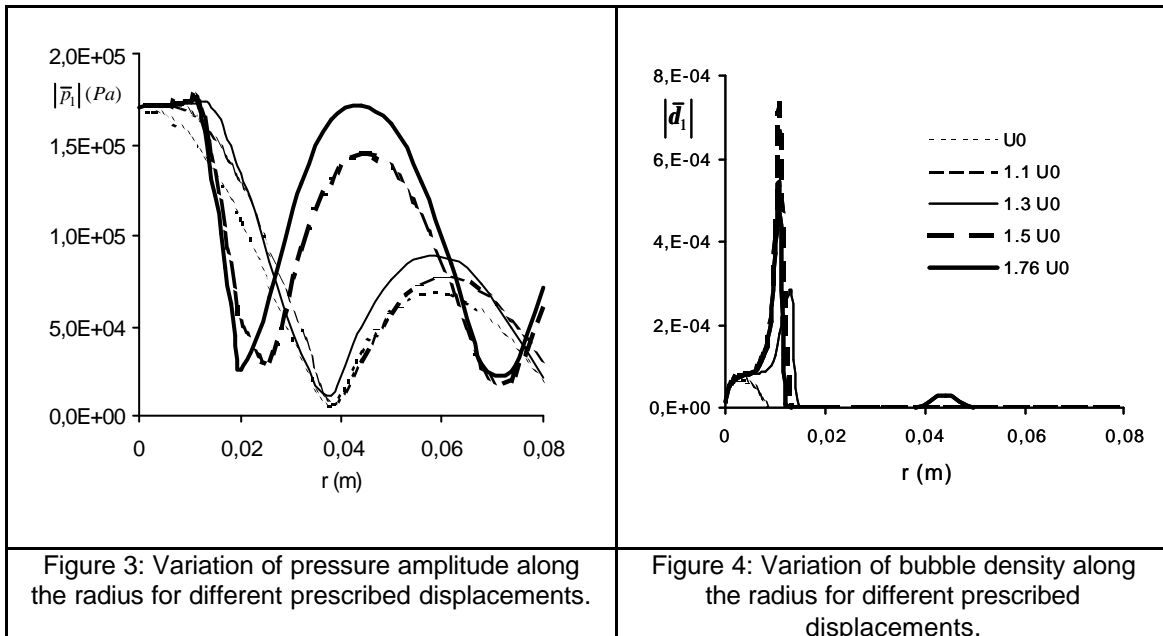
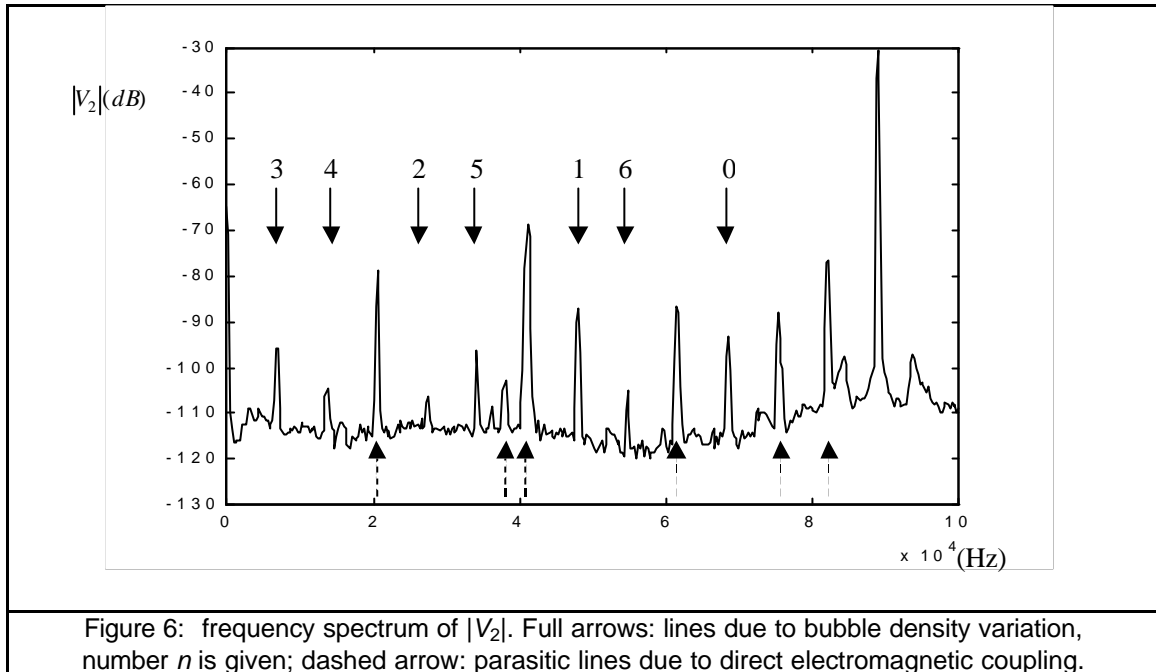


Figure 5: Set-up for measurement of local variation of fluid electrical impedance



ACKNOWLEDGEMENTS

This work was supported by CNRS and CSIC (French-Spanish cooperation project #7967) and by the European Union (Feder-Retex II).

BIBLIOGRAPHICAL REFERENCES

- [1] O. Louisnard, *Contribution à l'étude de la propagation des ultrasons en milieu cavitant*, PhD Thesis, Ecole des Mines de Paris, (1998).
- [2] S. Dähnke, K.M. Swamy, F.J. Keil, *Modeling of three-dimensional pressure fields in sonochemical reactors with inhomogeneous density distribution of cavitation bubbles. Comparison of theoretical and experimental results*, *Ultras. Sonochem.* 6, 31-41, (1999).
- [3] G. Servant, J.-P. Caltagirone, A. Gérard, J.-L. Laborde, A. Hita, *Numerical simulation of cavitation bubble dynamics induced by ultrasound waves in high frequency reactor*, *Ultras. Sonochem.* 7, 217-227, (2000).
- [4] M. Krömer, F.J. Keil, *Numerical modeling of non-linear sound propagation in cavitating sonoreactors*, *Proceedings of the 3rd Conference applications of Power Ultrasound in Physical and Chemical Processing*, 175-180, (2001).
- [5] R.E. Caflish, M.J. Miksis, G.C. Papanicolaou, L. Ting, *Effective equations for wave propagation in bubbly liquids*, *J. Fluid Mech.* 153, 259-273, (1985).
- [6] B. Dubus, O. Ledez, C. Granger, P. Mosbah, C. Campos-Pozuelo, *Numerical modeling of the ultrasonic cavitation field*, *Proceedings of the 3rd Conference applications of Power Ultrasound in Physical and Chemical Processing*, 169-174, (2001).
- [7] L.D. Rozenberg, *The cavitation zone*, in *High-intensity ultrasonic fields* ed. By L.D. Rozenberg, part VI, Plenum Press, (1971).
- [8] E.A. Neppiras, *Measurement of acoustic cavitation*, *IEEE Trans.on Sonics and Ultrason.* 15, 81, (1968).
- [9] L.S. Jacobsen, R.S. Ayre, *Engineering vibrations*, McGraw-Hill, (1958).
- [10] V.A. Akulichev, *Experimental investigation of an elementary cavitation zone*, *Sov. Phys. Ac.* 14, 284-289, (1969).
- [11] O.C. Zienkiewicz, *The finite element method*, 4th edition, McGraw-Hill, (1989).
- [12] ATILA, *Finite element code for piezoelectric and magnetostrictive transducer modeling, version 5.1.1, user's manual*, Institut Supérieur d'Electronique du Nord, Acoustics Laboratory, (1997).